

Dynamics of the intertropical convergence zone over the western Pacific during the Little Ice Age

Hong Yan^{1,2*}, Wei Wei³, Willie Soon⁴, Zhisheng An^{1,2}, Weijian Zhou^{1,2}, Zhonghui Liu⁵, Yuhong Wang¹ and Robert M. Carter⁶

Precipitation in low latitudes is primarily controlled by the position of the intertropical convergence zone, which migrates from south to north seasonally. The Little Ice Age (defined as AD 1400–1850) was associated with low solar irradiance and high atmospheric aerosol concentrations as a result of several large volcanic eruptions. The mean position of the intertropical convergence zone over the western Pacific has been proposed to have shifted southwards during this interval, which would lead to relatively dry Little Ice Age conditions in the northern extent of the intertropical convergence zone and wet conditions around its southern limit. However, here we present a synthesis of palaeo-hydrology records from the Asian–Australian monsoon area that documents a rainfall distribution that distinctly violates the expected pattern. Our synthesis instead documents a synchronous retreat of the East Asian Summer Monsoon and the Australian Summer Monsoon into the tropics during the Little Ice Age, a pattern supported by the results of our climate model simulation of tropical precipitation over the past millennium. We suggest that this pattern over the western Pacific is best explained by a contraction in the latitudinal range over which the intertropical convergence zone seasonally migrates during the Little Ice Age. We therefore propose that rather than a strict north–south migration, the intertropical convergence zone in this region may instead expand and contract over decadal to centennial timescales in response to external forcing.

Tropical rainfall varies in association with the seasonal migrations of the circum-global intertropical convergence zone (ITCZ) and the closely related monsoonal land–sea coupled systems. On millennial to orbital timescales, both palaeoclimate proxy research and climate modelling have suggested that the precipitation in the tropical and subtropical monsoon areas varies in parallel with latitudinal migration of the ITCZ, being characterized by opposing variations in the two hemispheres^{1–5}. With southward migration of the ITCZ, the precipitation in the Northern Hemisphere summer monsoon area decreases whereas the precipitation in the Southern Hemisphere summer monsoon area increases; and vice versa. Climate models suggest that the millennial to orbital timescale migration of the mean annual position of the ITCZ is related to changes in Northern Hemisphere high-latitude climate, the Atlantic meridional overturning circulation and the asymmetrical insolation input between hemispheres^{1–4,6}. A southward migration of the ITCZ occurs when the North Atlantic region is relatively cold owing to enhanced high-latitude ice cover and a slowdown of the Atlantic meridional overturning circulation^{1–3}. Conversely, a northward migration of the ITCZ mean position is usually driven by increased Northern Hemisphere insolation input relative to the Southern Hemisphere^{2,4,6}.

The dynamical variation of the ITCZ rainbelt has also been considered the main factor for centennial timescale hydrologic changes in tropical areas over the past millennium^{7,8}. A large body of palaeo-proxy evidence suggests that during the relatively cold Little Ice Age period (LIA, ~AD 1400–1850), regions located at the northern limit of the ITCZ rainbelt, including the pan-Caribbean

region^{6,9}, became drier relative to both the warm Medieval Climate Anomaly period (MCA, ~AD 800–1300) and the most recent 150 years, pointing to a possible southward shift of the ITCZ (refs 7,8). Meanwhile, some hydrologic records from the southern boundary of the ITCZ that reflect a wetter LIA are also evidence in support of southward migration of the ITCZ mean position^{8,10,11}.

Although a similar/parallel southward migration of the ITCZ has been described during the LIA in open ocean areas of the Pacific⁷, the pattern of change for the west Pacific marine–continental ITCZ remains less well established¹². In this study, we synthesized high-resolution palaeo-hydrology records from the East Asian–Australian summer monsoon regions during the past millennium to test the variation pattern of the west Pacific ITCZ. Surprisingly, we found that the west Pacific region has yielded a precipitation distribution pattern in contradiction to what would normally be predicted from the southward shift of the ITCZ mean position during the LIA. Instead of the expected pattern, both the East Asian Summer Monsoon (EASM) and the Australian Summer Monsoon (ASM) retreated synchronously during the LIA and the core precipitation zones converged more narrowly within the tropics.

Palaeo-hydrology records from the EASM area

Many studies, including those using speleothem records^{2,13–16}, lake sediment records^{12,17–19} and historical documentary records²⁰, have focused on describing the hydrologic changes in the EASM area over the past millennium, with the results showing obvious regional differences (Fig. 1 and Supplementary Figs 1 and 2). The palaeo-hydrology records from the northern limit of the EASM, including a lake sediment record (D1; ref. 18), a historical archive record (D2;

¹State Key Laboratory of Loess and Quaternary Geology, Institute of Earth Environment, Chinese Academy of Sciences, Xi'an 710061, China. ²Joint Center for Global Change Studies (JCGS), Beijing 100875, China. ³The Alfred Wegener Institute, Helmholtz Centre for Polar and Marine Research, Bremerhaven 27570, Germany. ⁴Harvard-Smithsonian Center for Astrophysics, Cambridge, Massachusetts 02138, USA. ⁵Department of Earth Sciences, University of Hong Kong, Hong Kong, China. ⁶Institute of Public Affairs, Melbourne, Victoria 3000, Australia. *e-mail: yanhong@ieecas.cn

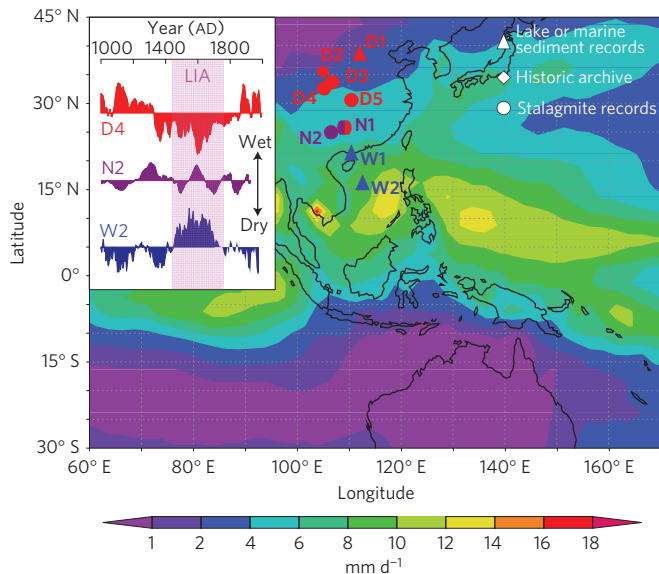


Figure 1 | Pattern of rainfall within the EASM region during the LIA.

The colour shading on the map indicates summer mean precipitation (from June to October) in the EASM area as derived from NCEP reanalysis2 from January 1979 to December 2010. Locations of proxy-hydrology records in the EASM area are indicated: D1 (ref. 18), D2 (ref. 20), D3 (ref. 13), D4 (ref. 14), D5 (ref. 15), N1 (ref. 2), N2 (ref. 16), W1 (refs 17,19) and W2 (ref. 12). Locations that were dry, without apparent change and wet during the LIA relative to the MCA/recent 150 years are marked in red, purple and blue, respectively. The three hydrologic conditions are objectively defined by the Relative Wet Index and *t*-test (see Methods for details). The time series of records D4, N2 and W2 are plotted in the inset.

ref. 20) and two stalagmite records (D3 and D4; refs 13,14), show similar variations over the past millennium and indicate that this region was hard hit by droughts during the LIA relative to the MCA and the past 150 years (Fig. 1 and Supplementary Fig. 1). Conversely, lake sediment records from the southern coast of China (W1 in Fig. 1 and Supplementary Fig. 2)^{17,19} and the northern South China Sea (W2 in Fig. 1 and Supplementary Fig. 2)¹² exhibit a clear wet condition during the LIA relative to the MCA and the past 150 years. At the same time, the hydrologic records located between these two regions reveal a gradual transition from dry to wet. The speleothem record (D5 in Fig. 1 and Supplementary Fig. 1)¹⁵ from central China reveals a moderate drought during the LIA whereas similar records (N1 and N2 in Fig. 1 and Supplementary Fig. 2)^{2,16} from southwest China, located near the transitional zone, show no significant difference between the LIA and the MCA. The spatial differences from north to south across China point to a probable retreat of the EASM during the LIA. This retreat led to reduced northward transport of monsoon moisture, a contracted core zone of precipitation, a relatively dry condition near the modern northern limit of the EASM and more precipitation in southern China during the LIA.

Palaeo-hydrology records from the ASM area

Hydrologic variations in the ASM area over the past millennium are less well established than those in the EASM area, but the retreat of the ASM during the LIA is still evident (Fig. 2 and Supplementary Figs 3, 4 and 5). The 1,000-year-long fluvial sedimentary records from the floodplain of Daly River (D11 in Fig. 2)²¹ and the Magela Creek Flood Plain (D12 in Fig. 2 and Supplementary Fig. 3)²¹ in the ‘Top End’ area of Australia suggest a reduced river discharge and dry conditions in this region during the LIA. Meanwhile, a nearby speleothem record provides further confirmation of dry conditions in tropical northwestern Australia during AD 1400–1700 (D13 in

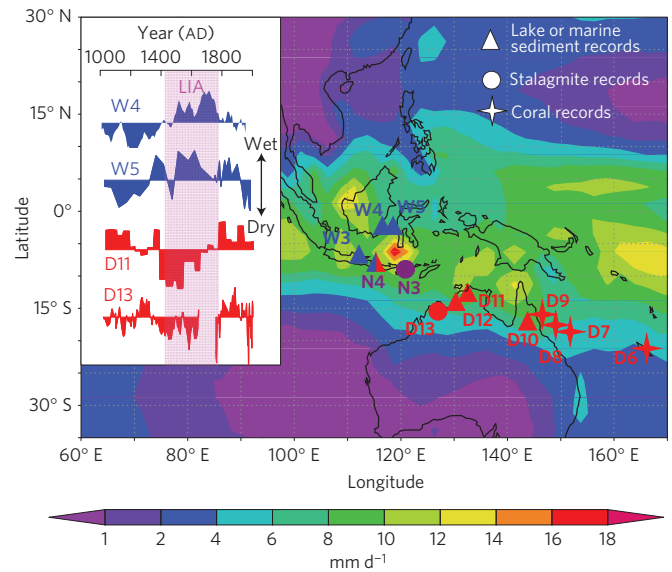


Figure 2 | Pattern of rainfall within the ASM region during the LIA.

The colour shading on the map indicates summer mean precipitation (from December to February) in the ASM area derived from NCEP reanalysis2 from January 1979 to December 2010. Locations of proxy-hydrology records in the ASM area are also indicated: D6 (refs 25,26), D7 (ref. 27), D8 (ref. 24), D9 (ref. 23), D10 (refs 28,29), D11 (ref. 21), D12 (ref. 21), D13 (ref. 22), N3 (ref. 31), N4 (ref. 32), W3 (ref. 30), W4 (ref. 10) and W5 (refs 8,11). Locations that were dry, without apparent change and wet during the LIA relative to the MCA/recent 150 years are marked in red, purple and blue, respectively. The time series of records W4, W5, D11 and D13 are plotted in the inset.

Fig. 2 and Supplementary Fig. 3)²². The more positive stalagmite $\delta^{18}\text{O}$ during the LIA relative to the MCA and the recent 150 years has been interpreted as indicating less precipitation in this region²².

The multi-proxy records from northeastern Australia also indicate dry conditions during the LIA (Supplementary Figs 3 and 4). The northeast tropical Queensland river flow and rainfall reconstruction derived from Great Barrier Reef coral luminescence studies (D9; ref. 23) clearly show less precipitation during the LIA than during the twentieth century. Meanwhile, all three seawater $\delta^{18}\text{O}$ records derived from coral $\delta^{18}\text{O}$ and Sr/Ca in Great Barrier Reef (D8; ref. 24), New Caledonia (D6; refs 25,26) and Flinders Reef (D7; ref. 27) exhibit more positive values (consistent with dry conditions) during the LIA than in the twentieth century. The dry LIA in northeastern tropical Australia has recently been further confirmed by two new peat humification records from Queensland (D10 in Fig. 2 and Supplementary Fig. 3), which document clearly that dry conditions prevailed during the LIA (refs 28,29). These records, together with the fluvial sedimentary and speleothem records from tropical western Australia, indicate that dry conditions probably covered the whole tropical Australian continent during the LIA.

In contrast to the drier conditions in northern Australia, several palaeo-hydrology records from the Indo-Pacific Warm Pool region, including the organic matter $\delta^{13}\text{C}$ record of lake sediment from Java (W3; ref. 30), a leaf wax δD record from Makassar Strait (W4; ref. 10) and the sea surface salinity record derived from $\delta^{18}\text{O}$ and Mg/Ca of planktonic foraminifera from Makassar Strait (W5; refs 8,11), consistently suggest more precipitation and wetter conditions during the LIA than that during the MCA/past 150 years (Fig. 2 and Supplementary Fig. 5). However, some hydrologic records from southern Indonesia, located between the Warm pool and northern Australia, show no clear dry or wet conditions during the LIA (refs 31–34). For example, the stalagmite $\delta^{18}\text{O}$ record from

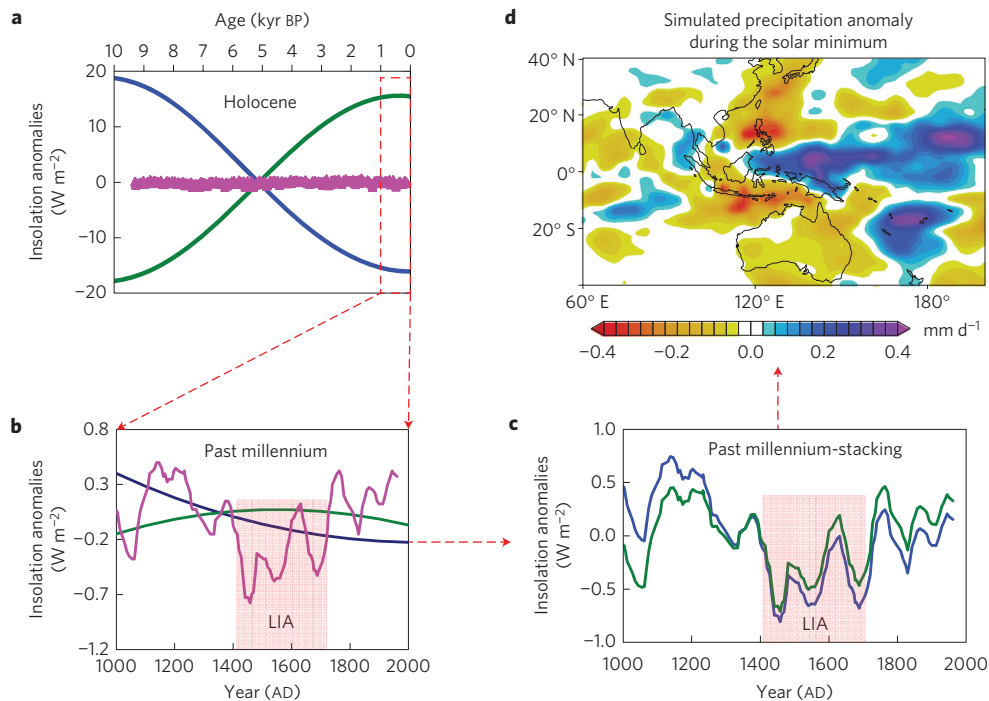


Figure 3 | Forcing and modelling results. **a, b**, Solar forcing representing the solar output (pink)^{37,38} and orbital parameters (blue and green lines are the July and January insolation at 23.5° N and 23.5° S, respectively)³⁶ during the Holocene (**a**, orbital changes dominating) and past millennium (**b**, solar output dominating). **c**, Total solar forcing at 23.5° N (blue) and 23.5° S (green) calculated by adding up the changes in the solar output and orbital parameters. **d**, Simulated annual mean precipitation anomaly during the late solar Maunder Minimum phase (AD 1690–1740) of the LIA with reference to the long-term mean (AD 1000–1800) in the MPI-ESM last millennial simulation⁴².

southern Indonesia shows no apparent difference between the LIA and the MCA or the most recent 150 years (N3 in Fig. 2 and Supplementary Fig. 5)³¹, whereas the δD of terrestrial plant wax indicates that rainfall has steadily increased in East Java over the past millennium (N4; ref. 32).

The general pattern of increased precipitation (LIA relative to MCA/recent 150 years) from northern Australia to the Indo-Pacific warm pool area is similar to that observed in the EASM area, and also consistent with a weakened ASM during the LIA.

Empirical explanation and climate modelling

The observed dry condition in the northern Australia monsoon area during the LIA argues against the established southward ITCZ migration hypothesis for the west Pacific region. It follows that the ITCZ migration theory, which was mainly proposed to explain millennial to orbital timescale tropical hydrologic changes^{1–4,6}, does not explain the documented decadal to centennial timescale hydrologic variations that occurred over the western Pacific region during the past millennium. Instead, we propose the alternative and more physically plausible hypothesis of a contraction of the ITCZ/monsoon zones during the LIA within the western Pacific, accompanied by a synchronized retreat of both the EASM and the ASM (Supplementary Figs 6 and 7).

Meanwhile, although the driving force of ITCZ migration on millennial to orbital timescale has been well described^{1–4,6}, the mechanism of the ITCZ dynamics on a decadal to centennial timescale (for example, the southward migration proposed for the LIA (ref. 7)) remains unclear^{7,12,35}. For example, a 5° southward ITCZ shift during the LIA was proposed by one previous study⁷, but the possible forcing factors for ITCZ migration, such as the freshwater input into the North Atlantic Ocean and orbitally driven asymmetrical insolation input between hemispheres (Fig. 3b), did not show marked changes during the LIA. In addition, a recent constraint suggests that a 5° southward shift would implicate a

large cross-equatorial atmospheric heat transport of 1.7 PW and an inter-hemispheric tropical sea surface temperature (SST) gradient (that is, 0°–20° N minus 0°–20° S) of 1.5 to 3.7 K, yet neither of which has been detected³⁵.

Solar insolation on the Earth depends not only on the orbital parameters³⁶ but also on the direct irradiance variations of the Sun³⁷. The precessional cycles of the equinoxes of Earth–Sun orbit have been demonstrated to be the most important orbital parameters that are linked with tropical hydrologic changes. The precessional forcing produces insolation anomalies that amplify the seasonality of insolation in one hemisphere at the expense of the other, thus resulting in opposite summer insolation variations between the Northern and Southern hemispheres (Fig. 3)³⁶. Hence more intense Northern Hemisphere summertime insolation favours an ITCZ that migrates farther north off the equator during the summer. In contrast to the precessional forcing, the intrinsic changes of solar irradiance are symmetrical and hence produce a synchronized forcing on both hemispheres³⁷. On the orbital timescale, the amplitude of insolation change caused by fluctuations of the orbital precessional cycle is much larger than that induced by variations in solar output (Fig. 3a)^{36,38}. For this reason, the ITCZ is expected to migrate north–south in phase with the changing inter-hemispheric insolation gradients. However, this situation reversed over the past millennium, during which period the insolation variation caused by orbital change became much smaller than that caused by fluctuations in direct solar irradiance (Fig. 3b and Supplementary Fig. 8)^{36,37}. The small variability of asymmetrical orbital insolation forcing during the past millennium seems too inadequate to cause large meridional migration of the ITCZ mean position during the LIA.

When adding the changes from both orbital parameters and solar irradiance, we have found that the insolation in the Northern and Southern hemispheres shows a similar variation pattern over the past millennium, with a decreased insolation during the LIA relative

to the MCA/past 150-year intervals (Fig. 3c and Supplementary Fig. 8). Such hemispherically symmetric forcing from intrinsic solar irradiance probably contributed to the synchronized retreats of both the EASM and the ASM during the LIA. On the other hand, large volcanic eruptions (that is, especially frequent and persistent volcanic activity around the tropical western Pacific region³⁹), may also yield symmetrical forcing between two hemispheres and could therefore also help to drive contractions of the monsoon/ITCZ belts. For example, some strong volcanic eruptions have been detected during the LIA (that is, coinciding with the Maunder Minimum and Dalton Minimum)^{39,40}.

Our proposal of a contracted monsoon–ITCZ in the Western Pacific region is also supported by published investigations of global monsoon precipitation in response to natural and anthropogenic forcings in the past millennium, based on simulations with the coupled ocean–atmosphere model ECHO-G (ref. 40). The simulated results suggest a symmetrical decrease in monsoon precipitation in both hemispheres during the LIA (see ref. 40 for details) with the three weakest periods around 1460, 1685 and 1800 (which respectively correspond to the deepest parts of the Spörer Minimum, Maunder Minimum, and Dalton Minimum intervals of reduced irradiance)⁴⁰, whereas the global monsoon strengthened nearly everywhere in the continental monsoon regions during the modelled MCA interval⁴⁰. Furthermore, the simulated precipitation increases in tropical Indonesia and rainfall decreases in northern Australia during the solar minima were also demonstrated in a recent idealized solar sensitivity experiment using the coupled climate model CCSM3 (ref. 41).

To analyse the impact of solar activity on tropical precipitation over the past millennium independently, we have also deployed the Coupled Model Intercomparison Project Phase 5 (CMIP5) style model from the Max Planck Institute Earth System Model (MPI-ESM) millennium simulation (see Supplementary Methods for details), using only solar variability as external forcing⁴². The model results (Fig. 3d), which show decreased precipitation in the west Pacific subtropical monsoon area of both hemispheres and more rainfall in the equatorial area during the periods of low solar activity, offer hints in support our proposal of a contracted monsoon/ITCZ in west Pacific during the LIA (Fig. 3d and Supplementary Fig. 9).

The simulated reduced global monsoon precipitation during the LIA was primarily attributed to reduced solar irradiance by Liu and colleagues⁴⁰. Our own simulation independently confirmed this result (Supplementary Fig. 9). Changes in the total amount of effective shortwave radiative forcing (that is, including short-term pulses of forcing from globally influential volcanic eruptions) can reinforce the thermal contrast between the continent and ocean (Table 3 in ref. 40), thereby resulting in centennial timescale variations in the global monsoon strength⁴⁰. Land has a much smaller heat capacity than ocean. When the effective radiative flux increases during the local summer, the land warming is much stronger than the warming of adjacent ocean and thus the thermal contrast between continent and ocean gets reinforced⁴⁰. This increased thermal contrast further enhances the pressure differences between land monsoon regions and the surrounding oceans (Table 3 in ref. 40) and therefore strengthens the monsoon circulation and its associated rainfall⁴⁰. A decrease in irradiance during the LIA, plus the unique land–sea distribution in the west Pacific region, would thus produce the decreased seasonal extremes of the monsoon moisture transport and the consequent contraction of the west Pacific monsoon/ITCZ.

It is worth noting that the model results also implied an increased zonal precipitation contrast between the east and west tropical Pacific during the LIA (Supplementary Fig. 9 and ref. 40), which would probably manifest itself as an enhanced Pacific Walker circulation. Although some temperature reconstructions proposed

an El Niño-like SST pattern in the tropical Pacific during the LIA (refs 43,44), the hydrologic studies, based on either proxy records^{10–12,45} or model simulations⁴⁶, present a clear strengthening of Pacific Walker circulation during the LIA, which should result in more precipitation in the Indo-Pacific warm-fresh pool region (see Supplementary Information for further discussion). That is to say, the scenario of a contracted western Pacific monsoon/ITCZ and an enhanced Pacific Walker circulation probably coexisted during the LIA interval, with both mechanisms contributing extra precipitation to the warm pool region.

Our main findings highlight the difficulty of applying the conventional interpretation of ITCZ migration to explain the hydrologic changes in the East Asian–Australian monsoon area that are known to have occurred during the past millennium. It remains the case, however, that the detailed position of the west Pacific monsoon/ITCZ during the LIA, the range of the ITCZ–monsoonal meridional contraction (locally or globally) and the mechanism of the contractions that have occurred are still not fully understood. Developing an enhanced understanding of this topic requires the collection of further high-resolution palaeo-hydrology proxy data, and the application of insightful and focused climate modelling studies.

Methods

Definition of the MCA and the LIA. To investigate the hydrologic changes between the MCA and the LIA, we have defined these terms as represented by distinct three-century-long intervals. The medieval interval, which is usually defined from AD 800 to 1300 in previous studies⁴⁷, has here been defined from AD 1000 to 1300 because we mainly focused on the past millennium. Correspondingly, a three-century-long LIA has been defined from AD 1400 to 1700, based on the minimum of the solar activity³⁷. The Welch's *t*-test result suggested a significant difference in solar irradiance forcing between AD 1400–1700 and AD 1000–1300.

Dry/wet conditions between the LIA and the MCA/recent 150 years. Proxy records from the Asia–western Pacific–Australia monsoon areas were selected to investigate the hydrologic changes between the LIA and the MCA/recent 150 years based on three main criteria. First, the temporal resolution of the data is better than 50 years and sufficient to distinguish among the MCA–LIA–recent 150-year intervals. Second, the dating error of the record is less than 100 years. Third, the proxy record has been used to reflect precipitation/humidity/monsoon variation in the original reference. Both the Relative Wet Index (RWI) and *t*-test were used to define and compare the dry/wet conditions between the LIA and the MCA/recent 150 years. The RWI and *t*-test were performed as follows:

RWI: The RWI between the LIA and the MCA for each proxy record was defined by calculating the RWI = (mean value during the LIA minus mean value during the MCA)/standard deviation. This method is also used to calculate the RWI between the LIA and the most recent 150 years. The time spans of the four coral records were too short to calculate the RWI between the LIA and the MCA. Thus we calculated the RWI only between the LIA and the most recent 150 years, the RWI being modified as RWI = (mean value before AD 1850 minus mean value after AD 1850)/standard deviation. Before the calculation, the resolution of each proxy record was adjusted to one year using linear interpolation. The calculated RWI values are given in Supplementary Table 1.

***t*-test:** The significance of the difference between the LIA and the MCA/recent 150 years for each hydrologic series was evaluated by applying an unpaired Welch's *t*-test, which does not require equal variance. Before the calculation, the effective sample size of the *t*-test was adjusted following the method in previous studies^{48,49} (see the next section, Correlation analysis, for details). The calculated *p* values are given in Supplementary Table 1. A *p* value less than 0.05 is considered statistically significant.

If the RWI between the LIA and the MCA is greater than 50% and the *p* value of the *t*-test is less than 0.05, a wet LIA relative to the MCA is defined. If the RWI between the LIA and the MCA is less than –50% and the *p* value of the *t*-test is less than 0.05, then a dry LIA relative to the MCA is defined. If the *p* value of the *t*-test is more than 0.05 or the RWI between the LIA and the MCA is between –50% and 50%, no apparent precipitation change is defined between the LIA and the MCA. This method was also used to define the dry/wet conditions between the LIA and the recent 150 years. Locations that were dry, had no apparent change or were wet during the LIA relative to the MCA/recent 150 years are coloured red, purple and blue in all map figures, respectively. If the dry/wet condition between the LIA and the MCA is different from the dry/wet condition between the LIA and the most recent 150 years, then a combined

colour is used. For example, the record N1 has no apparent change during the LIA relative to the MCA and a dry LIA relative to the most recent 150 years. Thus N1's label has purple left and red right.

Correlation analysis. For two time series, X and Y , the Pearson correlation coefficient r_{xy} was calculated as

$$r_{xy} = \frac{\sum_{i=1}^n (x_i - \bar{x})(y_i - \bar{y})}{(n-1)s_x s_y}$$

where n is the sample number, \bar{x} and \bar{y} are the sample means of X and Y , and s_x and s_y are the sample standard deviation of X and Y . For two time series (X and Y) with smoothing, we have to consider and adjust the autocorrelation in X and Y by using the effective sample size or the effective number of independence values. Following refs 48,49, we first calculated τ , the time between independent values (or the time to obtain a new degree of freedom) according to the following equation⁵⁰:

$$\tau = 1 + 2 \sum_{l=1}^{(n-1)} r_{xl} r_{yl}$$

where r_{xl} and r_{yl} are the autocorrelation at lag l for X and Y . The effective number of independence values was calculated as $n_{\text{eff}} = n/\tau$, and the Student t -value for assessing significance was calculated as

$$t = \frac{r_{xy} \sqrt{n_{\text{eff}} - 2}}{\sqrt{1 - r_{xy}^2}}$$

Received 16 June 2014; accepted 29 January 2015;
published online 9 March 2015

References

- Chiang, J. C. & Bitz, C. M. Influence of high latitude ice cover on the marine intertropical convergence zone. *Clim. Dynam.* **25**, 477–496 (2005).
- Wang, Y. J. *et al.* The Holocene Asian monsoon: Links to solar changes and North Atlantic climate. *Science* **308**, 854–857 (2005).
- Zhang, R. & Delworth, T. L. Simulated tropical response to a substantial weakening of the Atlantic thermohaline circulation. *J. Clim.* **18**, 1853–1860 (2005).
- Timmermann, A., Lorenz, S., An, S., Clement, A. & Xie, S. The effect of orbital forcing on the mean climate and variability of the tropical Pacific. *J. Clim.* **20**, 4147–4159 (2007).
- Schneider, T., Bischoff, T. & Haug, G. H. Migrations and dynamics of the intertropical convergence zone. *Nature* **513**, 45–53 (2014).
- Haug, G., Hughen, K., Sigman, D., Peterson, L. & Rohl, U. Southward migration of the intertropical convergence zone through the Holocene. *Science* **293**, 1304–1308 (2001).
- Sachs, J. P. *et al.* Southward movement of the Pacific intertropical convergence zone AD 1400–1850. *Nature Geosci.* **2**, 519–525 (2009).
- Newton, A., Thunell, R. & Stott, L. Climate and hydrographic variability in the Indo-Pacific Warm Pool during the last millennium. *Geophys. Res. Lett.* **33**, L19710 (2006).
- Hodell, D. A. *et al.* Climate change on the Yucatan Peninsula during the Little Ice Age. *Quat. Res.* **63**, 109–121 (2005).
- Tierney, J., Oppo, D., Rosenthal, Y., Russell, J. & Linsley, B. Coordinated hydrological regimes in the Indo-Pacific region during the past two millennia. *Paleoceanography* **25**, PA1102 (2010).
- Oppo, D. W., Rosenthal, Y. & Linsley, B. K. 2,000-year-long temperature and hydrology reconstructions from the Indo-Pacific warm pool. *Nature* **460**, 1113–1116 (2009).
- Yan, H. *et al.* South China Sea hydrological changes and Pacific Walker Circulation variations over the last millennium. *Nature Commun.* **2**, 293 (2011).
- Tan, L. *et al.* Centennial-to decadal-scale monsoon precipitation variability in the semi-humid region, northern China during the last 1860 years: Records from stalagmites in Huangye Cave. *Holocene* **21**, 287–296 (2010).
- Zhang, P. Z. *et al.* A test of climate, Sun, and culture relationships from an 1810-year Chinese Cave Record. *Science* **322**, 940–942 (2008).
- Hu, C. *et al.* Quantification of Holocene Asian monsoon rainfall from spatially separated cave records. *Earth Planet. Sci. Lett.* **266**, 221–232 (2008).
- Qin, J. *et al.* High resolution stalagmite records of climate change since 800 AD in Libo, Guizhou [In Chinese with English abstract]. *Carsologica Sinica* **27**, 266–272 (2008).
- Chu, G. *et al.* The 'Medieval Warm Period' drought recorded in Lake Huguangyan, tropical South China. *Holocene* **12**, 511–516 (2002).
- Liu, J. B. *et al.* Humid Medieval Warm Period recorded by magnetic characteristics of sediments from Gonghai Lake, Shanxi, North China. *Chin. Sci. Bull.* **56**, 2464–2474 (2011).
- Zeng, Y. *et al.* The wet Little Ice Age recorded by sediments in Huguangyan Lake, tropical South China. *Quat. Int.* **263**, 55–62 (2011).
- Tan, L. C., Cai, Y. J., Yi, L., An, Z. S. & Ai, L. Precipitation variations of Longxi, northeast margin of Tibetan Plateau since AD 960 and their relationship with solar activity. *Clim. Past* **4**, 19–28 (2008).
- Wasson, R., Bayliss, P. & Clelland, S. in *Symp. 4: Climate Change* (ed. Winderlich, S.) Kakadu National Park Landscape Symposia Series 2007–2009, Internal Report 567 (Supervising Scientist Division, Australian Government, 2010).
- Denniston, R. F. *et al.* A Stalagmite record of Holocene Indonesian-Australian summer monsoon variability from the Australian tropics. *Quat. Sci. Rev.* **78**, 155–168 (2013).
- Lough, J. M. Great Barrier Reef coral luminescence reveals rainfall variability over northeastern Australia since the 17th century. *Paleoceanography* **26**, PA2201 (2011).
- Hendy, E. *et al.* Abrupt decrease in tropical Pacific sea surface salinity at end of Little Ice Age. *Science* **295**, 1511–1514 (2002).
- DeLong, K. L., Quinn, T. M., Taylor, F. W., Shen, C.-C. & Lin, K. Improving coral-based paleoclimate reconstructions by replicating 350 years of coral Sr/Ca variations. *Palaeogeogr. Palaeoclimatol. Palaeoecol.* **373**, 6–24 (2013).
- Quinn, T. M. *et al.* A multicentury stable isotope record from a New Caledonia coral: Interannual and decadal sea surface temperature variability in the southwest Pacific since 1657 AD. *Paleoceanography* **13**, 412–426 (1998).
- Calvo, E. *et al.* Interdecadal climate variability in the Coral Sea since 1708 AD. *Palaeogeogr. Palaeoclimatol. Palaeoecol.* **248**, 190–201 (2007).
- Burrows, M. A., Fenner, J. & Haberle, S. G. Humification in northeast Australia: Dating millennial and centennial scale climate variability in the late Holocene. *Holocene* **24**, 1707–1718 (2014).
- Burrows, M., Fenner, J. & Haberle, S. Testing peat humification analysis in an Australian context: Identifying wet shifts in regional climate over the past 4000 years. *Mires Peat* **14**, 1–19 (2014).
- Rodysill, J. R. *et al.* A paleolimnological record of rainfall and drought from East Java, Indonesia during the last 1,400 years. *J. Paleolimnol.* **47**, 1–15 (2012).
- Griffiths, M. *et al.* Increasing Australian-Indonesian monsoon rainfall linked to early Holocene sea-level rise. *Nature Geosci.* **2**, 636–639 (2009).
- Konecky, B. L. *et al.* Intensification of southwestern Indonesian rainfall over the past millennium. *Geophys. Res. Lett.* **40**, 386–391 (2013).
- Rodysill, J. R. *et al.* A severe drought during the last millennium in East Java, Indonesia. *Quat. Sci. Rev.* **80**, 102–111 (2013).
- Hartmann, A. *et al.* Multi-proxy evidence for human-induced deforestation and cultivation from a late Holocene stalagmite from middle Java, Indonesia. *Chem. Geol.* **357**, 8–17 (2013).
- Donohoe, A., Marshall, J., Ferreira, D. & McGe, D. The relationship between ITCZ location and cross-equatorial atmospheric heat transport: From the seasonal cycle to the Last Glacial Maximum. *J. Clim.* **26**, 3597–3618 (2013).
- Laskar, J., Fienga, A., Gastineau, M. & Manche, H. La2010: A new orbital solution for the long-term motion of the Earth. *Astron. Astrophys.* **532**, A89 (2011).
- Bard, E., Raisbeck, G., Yiou, F. & Jouzel, J. Solar irradiance during the last 1200 years based on cosmogenic nuclides. *Tellus B* **52**, 985–992 (2000).
- Steinhilber, F., Beer, J. & Fröhlich, C. Total solar irradiance during the Holocene. *Geophys. Res. Lett.* **36**, L19704 (2009).
- Sigl, M. *et al.* Insights from Antarctica on volcanic forcing during the Common Era. *Nature* **4**, 693–697 (2014).
- Liu, J. *et al.* Centennial variations of the global monsoon precipitation in the last millennium: Results from ECHO-G model. *J. Clim.* **22**, 2356–2371 (2009).
- Steinke, S. *et al.* Mid to Late-Holocene Australian-Indonesian summer monsoon variability. *Quat. Sci. Rev.* **93**, 142–154 (2014).
- Jungclauss, J. H. *et al.* Climate and carbon-cycle variability over the last millennium. *Clim. Past* **6**, 723–737 (2010).
- Conroy, J. L., Overpeck, J. T. & Cole, J. E. El Niño/Southern Oscillation and changes in the zonal gradient of tropical Pacific sea surface temperature over the last 1.2 ka. *PAGES News* **18**, 32–34 (2010).
- Cobb, K. M., Charles, C. D., Cheng, H. & Edwards, R. L. El Niño/Southern Oscillation and tropical Pacific climate during the last millennium. *Nature* **424**, 271–276 (2003).
- Conroy, J. L., Overpeck, J. T., Cole, J. E., Shanahan, T. M. & Steinitz-Kannan, M. Holocene changes in eastern tropical Pacific climate inferred from a Galapagos lake sediment record. *Quat. Sci. Rev.* **27**, 1166–1180 (2008).
- Vecchi, G. A. *et al.* Weakening of tropical Pacific atmospheric circulation due to anthropogenic forcing. *Nature* **441**, 73–76 (2006).

47. Lamb, H. The early Medieval Warm Epoch and its sequel. *Palaeogeogr. Palaeoclimatol. Palaeoecol.* **1**, 13–37 (1965).
48. Trenberth, K. Signal versus noise in the Southern Oscillation. *Mon Weather Rev.* **112**, 326–332 (1984).
49. Bretherton, C. S., Widmann, M., Dymnikov, V. P., Wallace, J. M. & Blade, I. The effective number of spatial degrees of freedom of a time-varying field. *J. Clim.* **12**, 1990–2009 (1999).
50. Box, G. E. P., Jenkins, G. M. & Reinsel, G. C. *Time Series Analysis: Forecasting and Control* Vol. 16 (Holden-Day, 1976).

Acknowledgements

Financial support for this research was provided by the Ministry of Science and Technology of China, the Natural Science Foundation of China (41403018) and the Chinese Academy of Science.

Author contributions

H.Y. designed the study and wrote the manuscript. W.W. contributed to the section discussing climate model results. W.S. contributed significantly to improvements in the manuscript. Z.A., W.Z. and Z.L. contributed to discussion of the results and manuscript refinement. Y.W. and R.M.C. contributed to improving the English.

Additional information

Supplementary information is available in the [online version of the paper](#). Reprints and permissions information is available online at www.nature.com/reprints. Correspondence and requests for materials should be addressed to H.Y.

Competing financial interests

The authors declare no competing financial interests.